Does the elimination of ion pairs affect the thermal stability of cold shock protein from the hyperthermophilic bacterium *Thermotoga maritima*?

Nadine Frankenberg, Christine Welker, Rainer Jaenicke*

Institut für Biophysik und Physikalische Biochemie, Universität Regensburg, D-93040 Regensburg, Germany

Received 19 May 1999; received in revised form 12 June 1999

Abstract Cold shock proteins (Csps) from mesophiles and thermophiles differ widely in their stabilities, but show close structural similarity. Sequence variations involve mainly charged groups, supporting the view that ion pairs contribute significantly to the free energy of stabilization. Based on the known 3D structure of mesophilic *Bacillus subtilis* CspB and the modeled structure of hyperthermophilic Csp from *Thermotoga maritima* (*Tm*Csp), D9 and H61 of *Tm*Csp have been substituted by asparagine to find out whether the elimination of predicted ion pairs has a destabilizing effect. Thermal unfolding experiments show that the D9N mutant is destabilized by 9°C, whereas H61N exhibits unaltered wild type behavior. The results are in agreement with preliminary NMR data which confirm the predicted structure only for the N-terminal ion pair.

Key words: Cold shock protein; Hyperthermophile; Ion pair; Thermal stability; *Thermotoga*

1. Introduction

The question of what mechanisms of stabilization allow proteins from hyperthermophilic organisms to avoid thermal denaturation is currently in the center of intensive research. No general answer has yet been given. Comparisons of proteins from (hyper-)thermophiles and their mesophilic counterparts seem to indicate that any protein investigated so far has evolved its individual strategy [1]. Site-specific mutagenesis has been used successfully to unravel mechanisms of stabilization. In this connection, small proteins belonging to a highly conserved protein family such as cold shock proteins (Csps) may be considered ideal model systems. Since Csps from mesophiles and (hyper-)thermophiles differ only in a small number of amino acid residues, it seems most promising to make use of systematic or random mutagenesis in order to correlate increments of stabilization with specific amino acid substitutions. In this context, the most promising candidates seem to be ion pairs close to the protein surface [1,2].

Csps are monomeric cytosolic proteins consisting of less than 70 amino acids, without disulfide bonds or other post-translational modifications. Except for their high affinity to single-stranded DNA or RNA, nothing is known with respect to their biological function [3,4]. In spite of the fact that Csp from the hyperthermophilic bacterium *Thermotoga maritima* (*Tm*Csp) shows 76% sequence homology (61% identity) to Csp from the mesophilic *Bacillus subtilis* (CspB), its thermal stability ($T_m = 87°C$) exceeds that of CspB by 35°C [5]. Homology modeling of the spatial structure of *Tm*Csp (based on the known X-ray structure of CspB) allows a number of charged residues to be selected which were used to screen optimum candidates for site-directed mutagenesis experiments. Taking advantage from the sequence alignment and the tentative 3D structure, all the basic residues (R2, K11, K41, K54, H61) and the acidic residues (D9, E33, E47) turn out to be located close to the surface of the protein (cf. [5–7]). Some of them seem to be candidates for ion clusters: for example, D9, K11/K12 may form a salt bridge, or E33, E47, H61, E49 and K63 may be arranged such that the distances between the positive and negative charges are below 5 Å (Fig. 1). After careful inspection of the modeled structure, D9 and H61 were selected to find out what is the effect when either of these two residues is substituted by the corresponding amino acid in CspB using site-directed mutagenesis. Since more substitutions are planned, the intein technique was applied in order to produce the mutant proteins [8].

2. Materials and methods

2.1. Cloning and expression

Escherichia coli strains DH10b (Bethesda Research Laboratories) and BL21(DE3) (Novagen) were used for cloning and expression. The *Tm*Csp gene was cloned into the vector pet21int, i.e. a pet21a vector (Novagen) containing a modified *Saccharomyces cerevisiae* VMA-I intein and a *Bacillus circulans* chitin binding domain (New England Biolabs) providing a T7 promoter system for high expression levels in *E. coli*. Cells were grown in Luria-Bertani medium at 15°C to $OD_{546nm} = 2$, and induced by adding IPTG to a final concentration of 1 mM. After incubation at 15°C for 24 h, the cells were spun down and the pellet resuspended in 20 mM Na-phosphate, 1 mM EDTA, 500 mM NaCl, pH 7.5 (buffer A) containing 5 mM $MgCl_2$, 20 μg/ml DNase I and RNase A, and then disrupted in a French press at 1.0–1.2×10^8 N/m^2. The supernatant of a 30 min centrifugation at $48\,000 \times g$ was applied to a 10 ml chitin column equilibrated with buffer A. After washing with 10 volumes of buffer A, the fusion protein was cleaved by adding dithiothreitol (DTT) to a final concentration of 50 mM directly to the chitin resin. One hour at room temperature was sufficient to cleave the fusion protein completely. Csp was finally eluted with 20 mM Na-phosphate, 1 mM EDTA, 50 mM NaCl, pH 7.5 (buffer B). Regeneration of the column was performed with three volumes of buffer B containing 1% sodium dodecyl sulfate, followed by five volumes of water. Csp-containing fractions were pooled, dialyzed to remove DTT and applied to a Resource Q-column (Pharmacia) equilibrated with buffer B to remove impurities of nucleic acids. The flow-through contained Csp; the nucleic acids were eluted by 20 mM Na-phosphate, 1 mM EDTA, 1 M NaCl, pH 7.5 (buffer C).

2.2. Mutagenesis

Site-directed mutagenesis made use of the QuikChange kit of Stratagene and the following oligonucleotide primers (mismatches are in bold letters, *Bsa*AI and *Bst*BI restriction sites are underlined):

Mutant H61N: 5′-GAA AGG TCC ACA GGC AGC G**AA CGT** GAA AGT AGT TGA GCC CGG G-3′ and 5′-CCC GGG CTC AAC TAC TTT **CAC GTT** CGC TGC CTG TGG ACC TTT C-3′.

*Corresponding author. Fax: (49) (941) 943 2813.
E-mail: rainer.jaenicke@biologie.uni-regensburg.de

PII: S0014-5793(99)00829-7

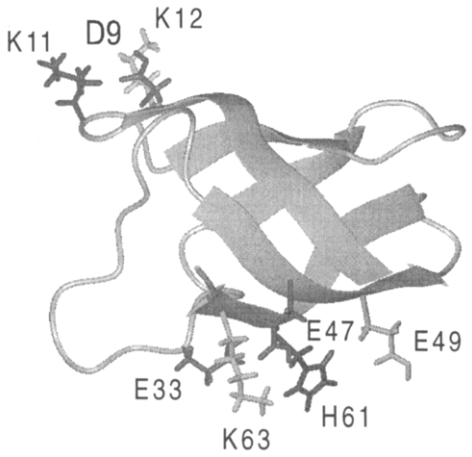

Fig. 1. Homology model of *Tm*Csp on the basis of the *B. subtilis* NMR structure. Modeling was performed using MODELLER versions 3 and 4.

Mutant D9N: 5′-GAG AGG AAA GGT TAA GTG GTT CAA TTC GAA GAA GGG CTA CGG ATT C-3′ and 5′-GAA TCC GTA GCC CTT CTT CGA ATT GAA CCA CTT AAC CTT TCC TCT C-3′. The mutations were confirmed by restriction digest and sequencing.

2.3. Spectroscopic characterization

UV absorption was measured in 20 mM Na-phosphate pH 7.5 in a Kontron Uvikon 391 spectrophotometer. Protein concentrations (C_{Csp}) were determined based on the specific absorption coefficient, 1.72 ml mg^{-1} cm^{-1} for *Tm*Csp [7] and 1.68 ml mg^{-1} cm^{-1} for $TmCsp_{int}$ and the mutants [9]. Fluorescence emission spectra of native and denatured (6 M GdmCl) protein were monitored in 100 mM Na-cacodylate buffer pH 7.0 at $\lambda_{exc} = 280$ nm, using a Spex FluoroMax-2 fluorescence spectrograph. CD spectra in the far- and near-UV were recorded in a Jasco J715 CD spectropolarimeter at $C_{Csp} = 140$ and 350 μg/ml in 20 mM Na-phosphate pH 7.0 and in 100 mM Na-cacodylate buffer pH 7.0, respectively.

2.4. Equilibrium unfolding

GdmCl-induced equilibrium unfolding was monitored by fluorescence emission at 337 nm in a Perkin Elmer MPF-L3 fluorescence spectrograph; $C_{Csp} = 10$ μg/ml. Data were analyzed according to Santoro and Bolen [10].

Temperature-induced unfolding transitions were recorded at 5–105°C by changes in the far-UV CD signal at 215 nm in 100 mM Na-cacodylate buffer pH 7.0; $C_{Csp} = 400$ μg/ml. Samples were overlaid with mineral oil and heated twice: first at 1 K/min, then at 0.5 K/min. Data were analyzed according to Swint and Robertson [11].

2.5. Unfolding and folding kinetics

Unfolding and folding kinetics were measured in a DX.17MV stopped-flow spectrometer (Applied Photophysics), making use of the change in fluorescence above 300 nm at $\lambda_{exc} = 280$ nm. Experiments were carried out in 100 mM Na-cacodylate buffer pH 7.0. Unfolding was initiated by diluting the native protein solution 11-fold with buffer containing varying C_{GdmCl}s to a constant final C_{Csp} of 10 μg/ml. To initiate refolding, unfolded protein in 5.5 M GdmCl was diluted using the same dilution scheme and protein concentration. Kinetics were repeated seven times; averaging and analysis as mono-exponential functions made use of the software provided by Applied Photophysics.

2.6. Global fits

To obtain the temperature dependence of the free energy of stabilization (ΔG vs T), GdmCl-induced equilibrium transitions were measured at varying temperatures and evaluated simultaneously with a temperature-induced unfolding transition. A global, non-linear fit of the complete dataset was carried out using the Levenberg-Marquardt algorithm in PROFIT 5.0 (Quansoft). Again, the analysis of the thermal and GdmCl-induced transitions made use of the procedures described by Santoro and Bolen [10] and Swint and Robertson [11]. Here, ΔG is expressed as a function of the melting temperature (T_m), the change of enthalpy due to protein unfolding at T_m (ΔH_m), and the heat capacity change accompanying protein unfolding (ΔC_P) according to

$$\Delta G(T) = \Delta H_m\left(1-\frac{T}{T_m}\right)-\Delta C_p\left[(T_m-T)+T\ln\left(\frac{T}{T_m}\right)\right] \quad (1)$$

The program was instructed to fit T_m, ΔH_m and ΔC_P to identical values for all datasets; the other parameters were allowed to be chosen individually. The errors in the measured values were estimated to be ±4% in GdmCl-induced (fluorescence) and ±200 deg cm^2 $dmol^{-1}$ in thermally induced (far-UV CD) transitions. Because the denatured baseline of thermal unfolding transitions of natural *Tm*Csp is very short, its slope was determined from a temperature-induced unfolding transition in 2 M GdmCl [7].

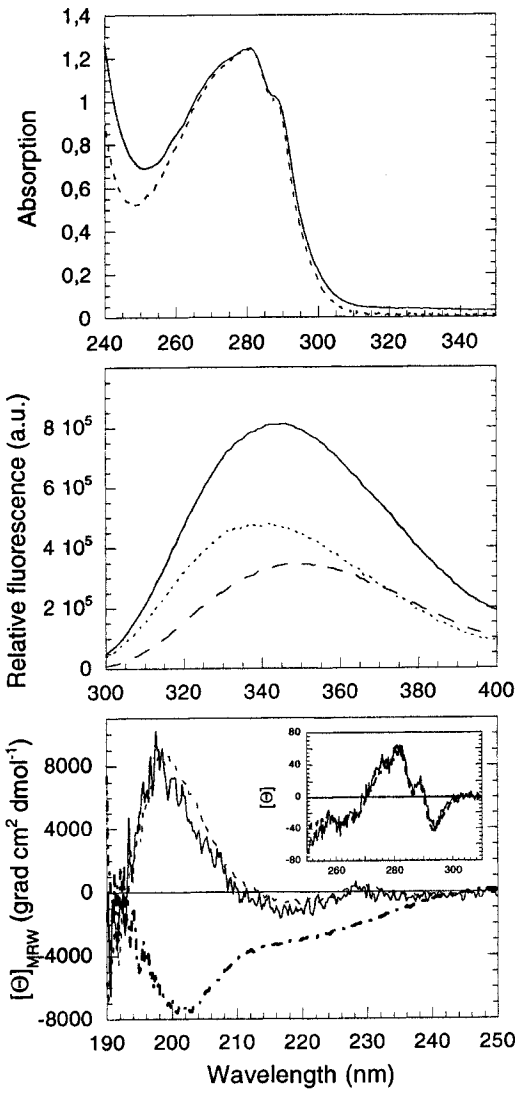

Fig. 2. Spectroscopic characterization of *Tm*Csp and D9N. Upper panel: UV absorption spectra of *Tm*Csp (dashed line) and D9N (solid line) in 20 mM Na-phosphate pH 7.5. Middle panel: Fluorescence emission spectra of native D9N (solid line) and D9N denatured in 6 M GdmCl (dashed line) in 100 mM Na-cacodylate pH 7.0; $C_{Csp} = 10$ μg/ml. Dotted line: fluorescence difference spectrum. Lower panel: Far-UV CD spectra of D9N (solid line) and *Tm*Csp (dashed line) at 20°C, and *Tm*Csp at 98°C (dot-dashed line) in 20 mM Na-phosphate pH 7.0; $C_{Csp} = 140$ μg/ml. Inset: Near-UV CD spectra of *Tm*Csp (dashed line) and D9N (solid line) in 100 mM Na-cacodylate pH 7.0; $C_{Csp} = 350$ μg/ml.

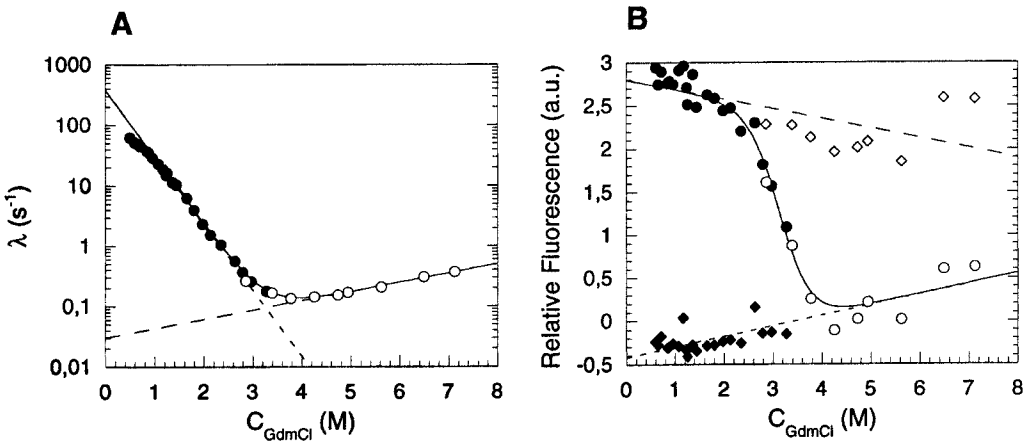

Fig. 3. Folding/unfolding kinetics of D9N. A: Apparent rate constants λ of folding (●) and unfolding (○) of D9N in 100 mM Na-cacodylate pH 7.0 at 25°C and C_{D9N} = 10 μg/ml. Fit on the basis of the two-state model (solid line), k_{NU} (dashed line) and k_{UN} (dotted line). B: Initial (◇, ◆) and final (○, ●) values of the folding (open symbols) and unfolding kinetics (closed symbols).

3. Results and discussion

3.1. Spectroscopic characterization

*Tm*Csp purified with the intein system (*Tm*Csp$_{int}$) contains two additional amino acids, proline and glycine, on its C-terminal end. In order to prove the authenticity of the extended form of the protein as well as its D9N and H61N mutants, their spectral characteristics were compared with those of natural *Tm*Csp [7]. The absorption, fluorescence and CD spectra of all four proteins were found to be identical. As an example, Fig. 2 illustrates the spectra of the D9N mutant. The UV absorption spectrum (Fig. 2, upper panel) shows a maximum at 280 nm with a tryptophan shoulder at 288 nm. The A_{280}/A_{260} ratio is 1.5; it is slightly below that of *Tm*Csp (1.6), probably due to an impurity of nucleic acids which is difficult to remove. The fluorescence emission spectra (Fig. 2, middle panel) of native D9N shows a maximum at 341 nm which is shifted to 349 nm upon chemical denaturation in 6 M GdmCl. Under this condition, the fluorescence intensity decreases to 40%. The far-UV and near-UV CD spectra (Fig. 2, lower panel) are also identical within experimental error, indicating that neither the secondary nor the tertiary structure of *Tm*Csp$_{int}$ and the mutants differs from wild type *Tm*Csp. The given findings are what one would expect, as there are no aromatic residues in the neighborhood of D9 and H61.

3.2. Stability of *Tm*Csp$_{int}$, H61N and D9N

Based on the spectral data (Fig. 2), the stability of *Tm*Csp$_{int}$ and its mutants was determined from GdmCl- and temperature-induced equilibrium unfolding transitions using fluorescence emission and far-UV CD. The denaturation profiles of Csp$_{int}$ and its H61N mutant were found to be identical and indistinguishable from that of *Tm*Csp (data not shown, cf. [7]). In the case of D9N, the GdmCl-induced equilibrium transition yields $\Delta G_{stab}(25°C) = 21.2 \pm 1.8$ kJ mol^{-1} and a cooperativity $m = -6.8 \pm 0.6$ kJ mol^{-1} M^{-1} [12], again in agreement with data reported for *Tm*Csp: $\Delta G_{stab}(25°C) = 21.7 \pm 1.1$ kJ mol^{-1} and $m = -6.7 \pm 0.2$ kJ mol^{-1} M^{-1} [6]. Stopped-flow kinetic experiments at 0.5–7.5 M GdmCl confirm the result. They show mono-exponential characteristics and allow the apparent rate constants of folding λ to be determined (Fig. 3A). Unfolding and refolding kinetics at the same GdmCl concentration led to identical λ values, indicating that the equilibrium is reached at the same rate, independent of whether the reaction is started from the native or the denatured protein. Except for the slight rollover at low C_{GdmCl}, the apparent rate constants depend linearly on C_{GdmCl}. Since two-state folding has been shown to be an inherent property of Csps [5], the rollover is ascribed to residual DNA or RNA binding rather than the formation of an intermediate on the folding pathway.

Using the microscopic rate constants for the two-state unfolding and refolding reactions (k_{NU} and k_{UN}) and their C_{GdmCl} dependence (m_{NU} and m_{UN}) in order to confirm the above equilibrium data ΔG and m can be calculated according to

$$\Delta G^{kin}_{stab} = -RT \ln(k_{UN}/k_{NU}) \text{ and } m^{kin} = RT\,(m_{NU} - m_{UN}) \quad (2)$$

The results for D9N are: $\Delta G^{kin}_{stab} = 23.4$ kJ mol^{-1} and $m^{kin} = -7.2$ kJ mol^{-1} M^{-1}, in close agreement with the data obtained for *Tm*Csp: $\Delta G^{kin}_{stab} = 23.5$ kJ mol^{-1} and $m^{kin} = -7.1$

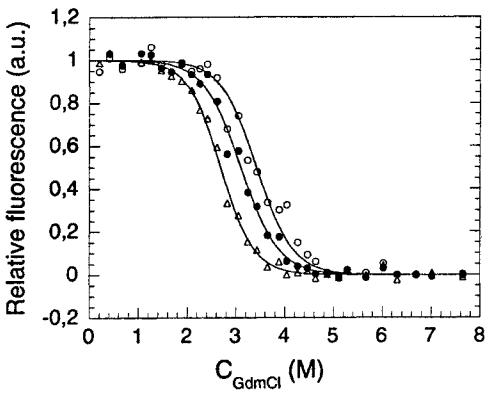

Fig. 4. GdmCl-induced equilibrium transitions of D9N at varying temperatures, monitored by the fluorescence emission at 337 nm in 100 mM Na-cacodylate pH 7.0; C_{Csp} = 10 μg/ml. In order to avoid crowding of symbols, only the profiles for 15°C (○), 25°C (●) and 35°C (△) are given. The transition curves belong to the global fit of the data.

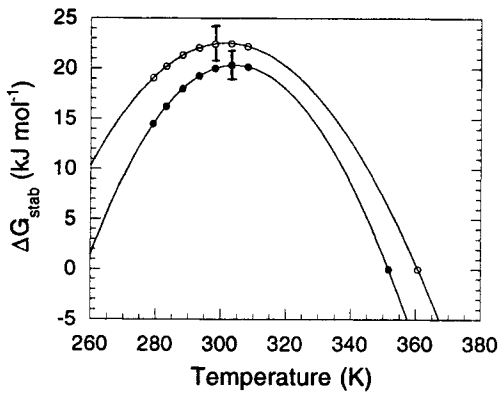

Fig. 5. Temperature dependences of the free energy of stabilization at 0 M GdmCl (ΔG_{stab}) of *Tm*Csp (○) and D9N (●) resulting from the global fit of the data, using PROFIT.

kJ mol^{-1} M^{-1} [6]. Evidently, there is no difference between wild type *Tm*Csp and the D9N mutant regarding their thermodynamic parameters. Initial and final values of folding and unfolding at varying C_{GdmCl}s are shown in Fig. 3B. The fact that they are identical over the whole transition range confirms the two-state model. The quantitative analysis yields $\Delta G_{stab} = 25.0 \pm 3.0$ kJ mol^{-1} and $m = -7.2 \pm 0.9$ kJ mol^{-1} M^{-1}, again in agreement with the above *Tm*Csp data.

As clearly shown by repeated heating at different heating rates, thermal denaturation of *Tm*Csp$_{int}$ and its mutants is fully reversible. Comparing the transition midpoints for D9N and *Tm*Csp$_{int}$, a significant decrease from 87 to 78°C is observed. The apparent discrepancy between this finding and the above thermodynamic data may be explained considering the temperature dependence of the free energy of stabilization which was gained from GdmCl-induced equilibrium transitions of D9N at 6, 10, 15, 20, 25, 30 and 35°C (Fig. 4). Over the whole range between 6 and 35°C, the transitions were fully reversible and followed the two-state model, as observed for *Tm*Csp [7]. Subjecting all data both from the GdmCl- and temperature-induced unfolding transitions to a global fit (see Section 2), D9N and *Tm*Csp yield the parabolic curves depicted in Fig. 5. Evidently, the stability profile for D9N exhibits a more pronounced curvature, corresponding to a higher change in heat capacity, $\Delta C_P = 5.7 \pm 0.7$ kJ mol^{-1} K^{-1} for D9N, compared to $\Delta C_P = 4.1 \pm 0.4$ kJ mol^{1} K^{-1} for *Tm*Csp [6] or 4.6 ± 0.4 kJ mol^{-1} K^{-1} [13]. The curve for D9N seems to be shifted to lower ΔG values; however, the deviation of the two profiles at temperatures below 330 K is within the range of error (see error bars at maximum ΔG_{stab}).

In conclusion, it is evident that D9N indeed lowers the thermal stability of *Tm*Csp significantly, whereas the substitution of H61 has no effect. Including at this point the information from the preliminary high-resolution NMR of *Tm*Csp, it turns out that the predicted structure from homology modeling is surprisingly good for the polypeptide backbone and the N-terminal region (including D9), whereas the C-terminal loop (around H61) is more extended so that the 5 Å limit of strong ion pairs does not hold (W. Kremer, S. Harrieder and H.R. Kalbitzer, personal communication). Thus, the present data support the ion pair hypothesis for a small, relatively unstable model protein. The complete high-resolution NMR analysis will provide a solid basis for choosing optimal candidates for a more detailed study.

Acknowledgements: Work was supported by the Deutsche Forschungsgemeinschaft and the Fonds der Chemischen Industrie. We thank Drs. U. Schmidt, G. Böhm and R. Rudolph for the plasmid. Fruitful discussions with Drs. W. Kremer and H.R. Kalbitzer are gratefully acknowledged.

References

[1] Jaenicke, R. and Böhm, G. (1998) Curr. Opin. Struct. Biol. 8, 738–748.
[2] Perutz, M.F. and Raidt, H. (1975) Nature 255, 256–259.
[3] Graumann, P. and Marahiel, M.A. (1998) Trends Biochem. Sci. 23, 286–290.
[4] Thieringer, H.A., Jones, P.G. and Inouye, M. (1998) BioEssays 20, 49–57.
[5] Perl, D., Welker, C., Schindler, T., Schröder, K., Marahiel, M.A., Jaenicke, R. and Schmid, F.X. (1998) Nature Struct. Biol. 5, 229–235.
[6] Welker, C. (1999) Ph.D. Thesis, University of Regensburg.
[7] Welker, C., Böhm, G., Schurig, H. and Jaenicke, R. (1999) Protein Sci. 8, 394–403.
[8] Perler, F.B. (1998) Cell 92, 1–4.
[9] Pace, C.N., Vajdos, F., Fee, L., Grimsley, G. and Gray, T. (1995) Protein Sci. 4, 2411–2423.
[10] Santoro, M.M. and Bolen, D.W. (1988) Biochemistry 27, 8063–8068.
[11] Swint, L. and Robertson, A.D. (1993) Protein Sci. 2, 2037–2049.
[12] Shortle, D. (1995) Adv. Protein Chem. 46, 217–247.
[13] Wassenberg, D., Welker, C. and Jaenicke, R. (1999) J. Mol. Biol. (in press).